Synthesis and Characterization of *Caladium bicolor*-Stabilized Iron Nanoparticle

Chukwudi Chidozie Aguomba [a], Remy Ukachukwu Duru [a*], Uche John Chukwu [a] and Chidi Obi. [a]

[a] Department of Pure and Industrial Chemistry, University of Port Harcourt, Rivers State, Nigeria.

Authors' contributions

This work was carried out in collaboration among all authors. All authors read and approved the final manuscript.

Original Research Article

ABSTRACT

Caladium bicolor samples were collected, thoroughly washed, shade dried, cut into small pieces, oven-dried and ground. Distilled water was added to the ground *C. bicolor* samples and heated. It was then filtered after heating, and the filtrate stored. To 0.05M solution of $FeCl_3$ was added the extract and stirred. The solution was then filtered and the residue oven dried. This synthesized NP was characterized with Differential scanning calorimetry (DSC), Thermogravimetric analysis (TGA), Braunauer-Emmett-Teller (BET) analysis, Scanning Electron Microscope (SEM) and X-ray diffraction (XRD) technique. The results from these analyses were characterised by attributes that indicated a successful synthesis of *Caladium bicolor*-incorporated Iron nanoparticles. Fourier transform infrared (FTIR) analysis was also carried out on the *Caladium bicolor* extract and synthesized NPs. Some of the results include O-H stretching (3291.50 cm^{-1}) which is characteristic

_____

*Corresponding author: E-mail: remy.duru@uniport.edu.ng;

of alcohol functional group. Alkane is suspected due to C-H stretching at 2919.20 cm^{-1} and alkene due to C=C stretching at 1628.11 cm^{-1}. Iron (III) chloride vibrations are suspected at 639.22 cm^{-1} (Fe-Cl stretching). DSC shows exothermic peaks at 323.6°C and 335.5°C and endothermic peaks at 105.7°C and 251.3°C. These results confirmed the presence of iron NPs. The use of plant extracts to synthesize nanoparticles (NP) has become increasingly desirable due to its low cost and non-toxic nature. *Caladium bicolor* fits this role because of its cheapness and not a food source for man or animals. Iron nanoparticles were synthesized using iron (III) chloride and *Caladium bicolor* extract.

Keywords: Caladium bicolor; nanoparticles; green; synthesis.

1. INTRODUCTION

Nanoparticles (NPs) are defined by the Organization for Standardization as structures whose sizes are within the range of 1 to 100 nm in at least one dimension. Nanoparticles can also be classified based on physical parameters such as electrical charge, chemical characteristics, shape and origin [1,2].
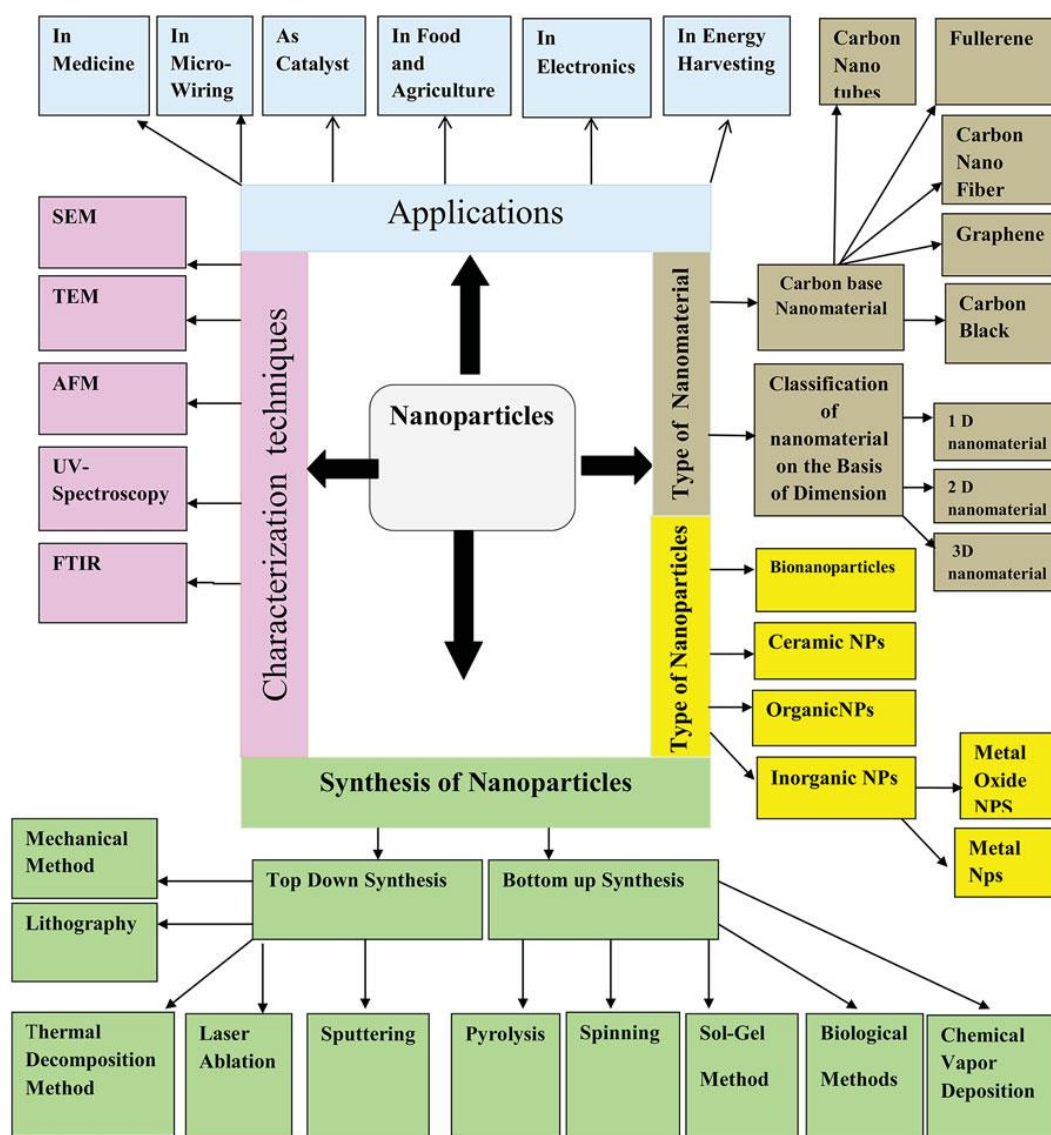
Fig. 1. Nanoparticle synthesis, types, characterization and usage [7]
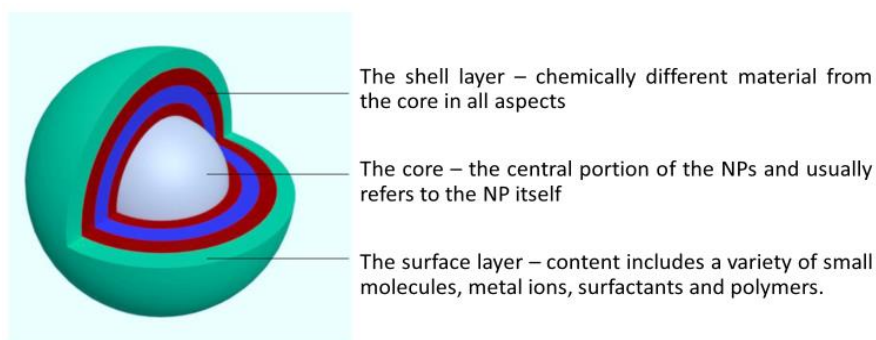
Fig. 2. Schematic of nanoparticle component-structured layers [8]

Nanoparticles chemistry is still an emerging discipline. Even though nanoparticles have been in use earlier on, the discipline only gained traction in the 1980s and 1990s. This was mostly due to the availability of electron microscopy and other characterization techniques [3].

Nanoparticles differ in many dimensions such as shapes and sizes. They can vary from zero dimensional where length, breadth and height are fixed at a single point e.g., nanodots to one dimensional where it possesses only one parameter such as graphene to two dimensional where it has length and breadth such as carbon nanotubes and even three dimensional where it has the three parameters of length, breadth and height like gold nanoparticle [4,5].

Nanoparticles have found several uses in history. There are also several ways of characterization and classification, several types and forms as shown in Fig. 1.

Nanoparticles possess a much higher surface-to-mass ratio than their bulk materials. This gives rise to surface atoms and surface energy contributing strongly to the material properties. This also impacts catalytic performance. Hence inactive bulk materials can become very active catalysts when produced as nanoparticles with high surface areas [6].

Mohamad et al. [8] listed the three (3) major layers of a nanoparticle as shown in Fig. 2. These are the outermost layer called the shell, the middle layer called the shell, and the innermost layer called the core.

1.1 Synthesis of Nanoparticles

Nanoparticle formation is a complex process that involves the fundamental stages of nucleation and growth within a reaction medium. This medium can exist in various states, including solid, liquid, gas, or plasma. While the growth mechanism typically follows a simple pathway, creating nanoparticles with intricate shapes requires a deeper understanding of the final stages of nucleation, characterized by well-defined, structured clusters [9].

To achieve precise control over nanoparticle size and shape, researchers employ different methods of synthesis. In gas-phase synthesis, critical parameters such as temperature, pressure, gas flow rates, and precursor concentrations are meticulously adjusted. Conversely, liquid-phase synthesis involves fine-tuning factors like precursor concentration, pH, temperature, and reaction time to govern nanoparticle dimensions.

The ability to tailor nanoparticle size and shape is crucial for unlocking their full potential in various applications. By grasping the underlying principles of nucleation and growth, scientists can design complex nanoparticle architectures with enhanced properties. The precise control offered by gas-phase and liquid-phase synthesis methods has far-reaching implications for fields such as catalysis, optoelectronics, biomedical imaging, and drug delivery [10].

Nanolization or nanoparticle formation or nanoparticle synthesis involves converting bulk materials or substances into their respective nanoparticles [11]. This can be achieved through the breakdown (top-down synthesis) of bulk materials into their nanoscale counterparts or the build-up (bottom-up synthesis) to form the desired nanomaterials.

There are two main approaches to nanoparticle synthesis. They are the top-down and bottom-up approaches as shown in Fig. 3.
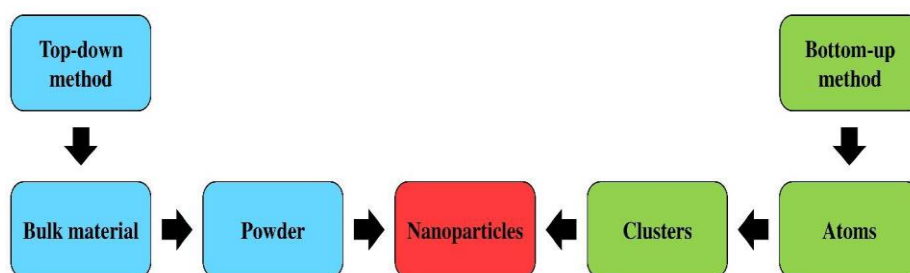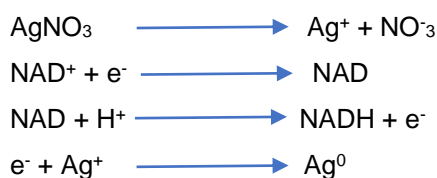
Fig. 3. NP Synthesis process schematic [4]

Synthesis of nanoparticles (NPs) may be achieved via physical, chemical and biological methods. Biological methods generally follow the "bottom-up" approach which involves the formation of the nanoparticles via the build up from small entities such as plant-derived biomolecules or ions by reduction and oxidation processes [12]. Bio-reduction of NPs takes place in-vitro or in-vivo. Enzymes, proteins, sugars and phytochemicals like phenolics, terpenoids, cofactors, flavonoids and phytochemicals act as reducing and stabilizing agents [13]. Green synthesis is mostly achieved via plant extracts. Green synthesis of NPs from its corresponding metal ion is environmentally friendly, free from chemical contamination, less expensive and safe for humans.

Plants are able to hyper-accumulate metals up to high concentrations. Extracts from *Desmodiumtriflorum* have been used to synthesize silver nanoparticles from aqueous silver nitrate at room temperature. The NPs were harvested by simple heat drying evaporation.

A possible mechanism for the reaction of silver ions is the reaction of glycolysis with $AgNO_3$.

$$AgNO_3 \longrightarrow Ag^+ + NO_3^-$$

$$NAD^+ + e^- \longrightarrow NAD$$

$$NAD + H^+ \longrightarrow NADH + e^-$$

$$e^- + Ag^+ \longrightarrow Ag^0$$

Nicotinamide adenine dinucleotide, NAD^+ which is a coenzyme in living cells is a strong reducing agent. As NAD^+, it accepts electrons from other molecules and becomes reduced. This forms NADH which donates electrons. Electron transfer reactions are the main function of NAD [14].

1.2 Nanoparticle Stabilizers and Modifiers

Nanoparticles are stabilized to enhance dispersion through electrostatic stabilization (adsorption of charged stabilizer molecules to the core metal and steric stabilization (coating the metal core with macromolecular stabilizers).

Agglomeration of metal nanoparticles which is thermodynamically favourable to NPs takes place in various ways namely;

1. Ostwald ripening (larger particles taking over smaller particles which are smaller than the critical size and this occurs during particle formation
2. arrested precipitation (facilitation of precipitation by formation of nucleation centers), and
3. direct inter-particle interactions. The inter-particle forces like van der Waals forces, magnetic dipolar interactions, and electric dipolar interactions are involved in these interactions [15].

1.3 Nanoparticle Characterization

There are several techniques for characterizing various features of NPs. They include X-Ray Diffraction (XRD), X-ray Photoelectron Spectroscopy (XPS), Fourier Transform Infra-Red (FTIR), Differential Scanning Calorimetry (DSC), Thermogravimetric analysis (TGA), Scanning Electron Microscopy (SEM), Transmission Electron Microscopy (TEM) and Brunauer-Emmett-Teller (BET).

2. MATERIALS AND METHOD

2.1 Sample Collection

Caladium bicolor whole plant samples were sourced from St. James Anglican Church grounds (4.94018ºN, 6.78228ºE), Rumuji village, Emohua Local Government Area of Rivers State, Nigeria. The samples were taken to the Herbarium of the Department of Plant Science and Biotechnology at the University of Port Harcourt where it was identified and authenticated.

Analytical grades of Iron (III) chloride, sodium borohydride, ethanol, nitric acid, hydrochloric acid, sodium hydroxide, distilled water and all other reagents were sourced from the store of the Department of Chemistry, University of Port Harcourt and JoeChem chemicals, Choba.

2.2 Equipment

Equipment used for the research include; Scanning electron microscope (SEM) – model PRO X, Phenonm World, 800-07334, Fourier transform infrared (FTIR) using FTIR micro-lab by Agilent Technologies, USA, X-ray diffraction (XRD) model - Philips Holland XRD system PW 1710, Thermogravimetric analysis (TGA) – model Shimadzu TG-60,Differential scanning calorimetry (DSC) – model Shimadzu DSC-50 system made by Shimadzu, Kyoto, Japan), Braunaur-Emmett-Teller (BET) – model St 2 on NOVA touch 4LX Quantachrome, stirring device, magnetic stirrer, water bath, radwag analytical balance, thermostat oven, block digestor, Taylor digestion tube, rotary evaporator, stop clock, pH meter, refrigerator.

2.3 Preparation of Samples

Samples of *Caladium bicolor* (whole plant) were washed several times under running water. These samples were later rinsed three times with distilled water to remove any remaining surface dirt. After shade-drying for two weeks to remove residual water, they were cut into small sizes. The cut samples were oven-dried at 60°C for 5 hours, ground to powder and stored in airtight containers.

2.4 Aqueous Extraction Process

Thirty grams of the ground samples of *C. bicolor* was added to 100 ml distilled water in a 250 ml conical flask. It was placed in a water bath and heated at 60°C for 30 minutes. It was filtered with Whatman No 24filter paper, filtrate was collected and stored at 4°C.

2.5 Preparation of 0.05M $FeCl_3$Solution

Distilled water (30 ml) was added to $FeCl_3$ (8.125 g) in a 250 ml conical flask was and stirred till totally dissolved. The mixture was transferred to a 1000 ml volumetric flask and made up to volume with distilled water.

2.6 Preparation and Biosynthesis of Nanoparticles

Caladium bicolor sample (10 ml) was added to 90 ml 0.05 M solution of $FeCl_3$in a 250 ml conical flask. This was stirred vigorously with a magnetic stirrer for 1 hour at room temperature. The resulting mixture was filtered with Whatman No 24 filter paper and oven-dried at 70°C for 10 hours.

3. RESULTS AND DISCUSSION

3.1 SEM

Fig. 4 has image with magnification of 1500x and scale bar of 0.5 µm. The microstructure of biosynthesized nanoparticles via aqueous extraction was observed. There was a significant particle size reduction and the nanoparticle was split into different layers of differing sizes. These SEM image shows morphology of synthesized iron nanoparticles. The presence of pores indicate agglomeration or a porous structure. The irregular shapes are due to the presence of organic compounds resulting from the *Caladium bicolor*. The high surface energy could also lead to aggregation. The larger pieces could be from unreacted iron ions from the iron (III) chloride.

3.2 X-ray Diffraction (XRD)

Figs. 5 and 6 show the X-ray diffraction patterns for the *Caladium bicolor* aqueous extract synthesized iron nanoparticle. The sharp XRD peaks indicate high crystalline nature of the synthesized nanoparticle resulting from size reduction. The high intensity peaks reflect that the reduced particle size of *Caladium bicolor* aqueous synthesized iron nanoparticle has more reactive sites than the bulk material. The XRD spectra of iron NP in Figs. 5 and 6 stabilized by *Caladium bicolor* displayed characteristic peaks at approximately 2θ = 44° and 82° corresponding to (110) and (211) planes, respectively. These results are in good agreement with the reference to the body-centered cubic structure of iron nanoparticle.

3.3 Differential Scanning Calorimetry (DSC)

Differential scanning calorimetry (DSC) thermogram in Fig. 7 shows two exothermic peaks at 323.6°C and 335.5°C. There are also two endothermic peaks at 105.7°C and 251.3°C. This DSC characterization of iron nanoparticles produced by *Caladium bicolor* whole plant extract indicates that the 323.6°C exothermic peak involves phase transitions. The 335.5°C exothermic peak of the sample at this temperature show thermal decomposition of the

sample. The endothermic peaks of 105.7°C and 251.3°C infer desorption and vaporization of the sample at these temperatures.

3.4 Braunauer-Emmett-Teller (BET)

The BET isotherm result is captured in Figs. 8 and 9. The surface area of the iron nanoparticles synthesized via *Caladium bicolor* whole plant extract was measured to be 10.15 m^2/g. The small surface area is attributable to agglomeration, pore structure, surface roughness, surface modification and particle shape. The slope of the linear BET isotherm (Fig. 9) is 600.571, intercept of 32.289 and correlation coefficient of 0.999751. Molecular weight of nitrogen is 28.013 gmol^{-1}. This low to medium range surface area is indicative that the synthesized nanoparticle is also suitable for applications like energy storage and drug delivery. They are also suitable for heavy metal and organics remediation from contaminated soil and wastewater, adsorbents and fillers in composites. This is typical of some iron nanoparticles like silicates, chlorides, and carbonates.
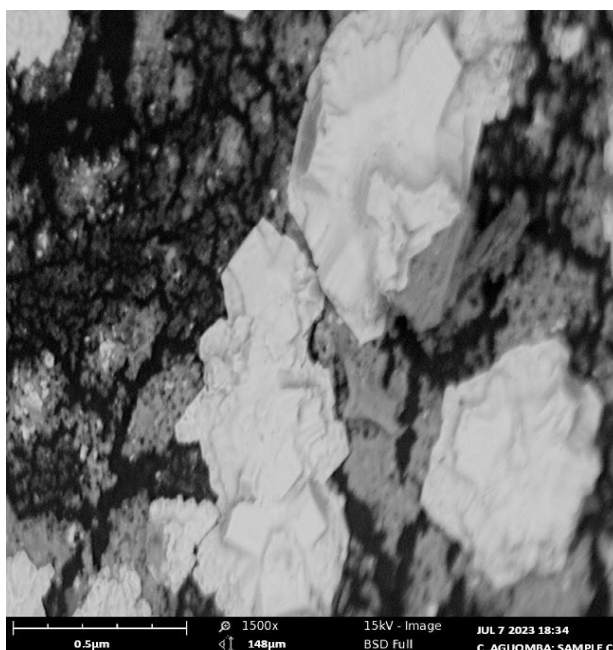
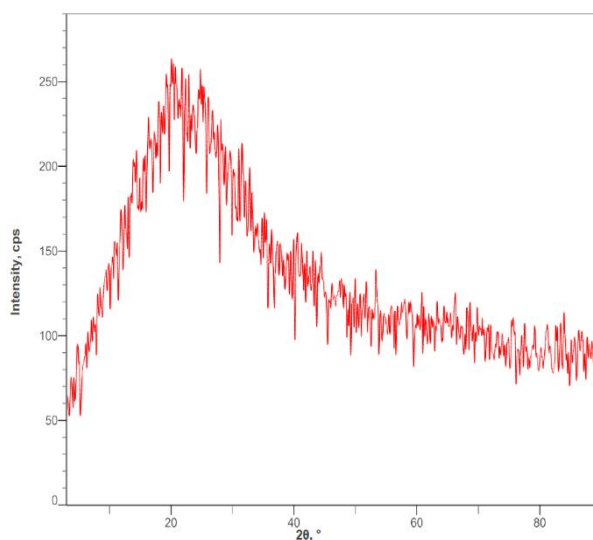

Fig. 4. SEM micrograph of iron NP
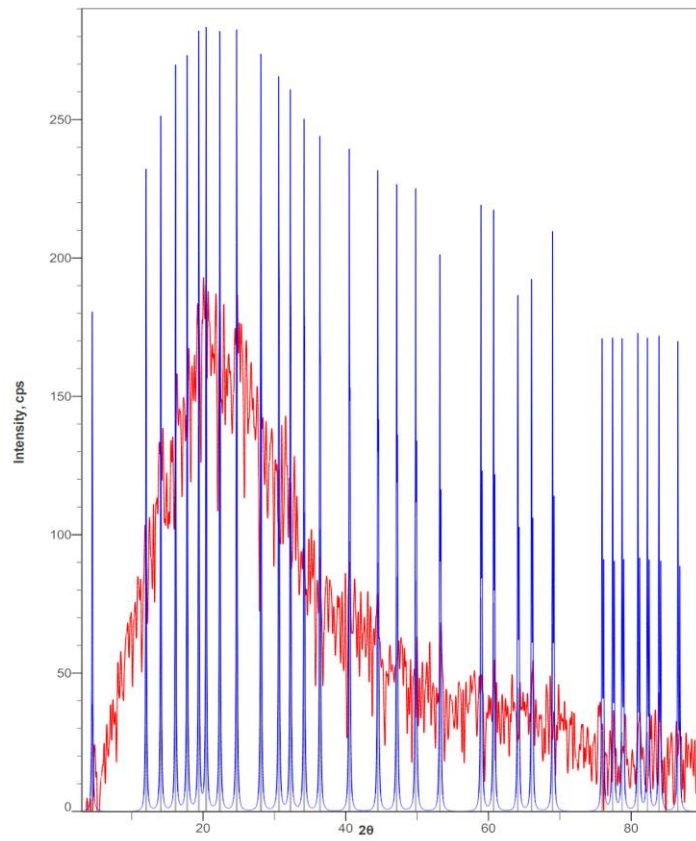

Fig. 5. XRD spectra of iron NP- a

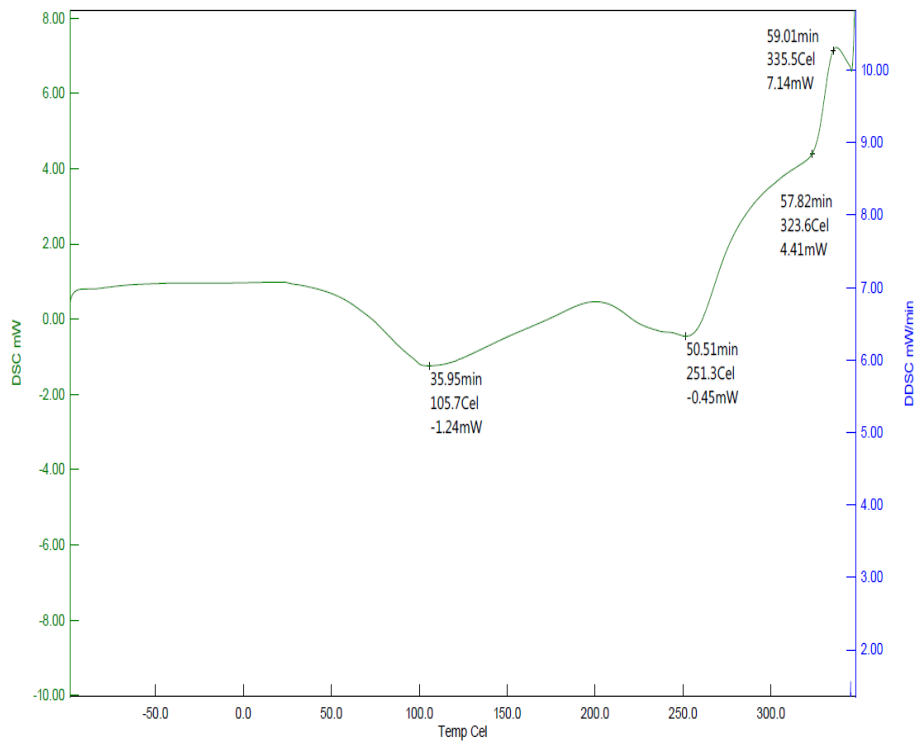**Fig. 6. XRD spectra of iron NP– b**
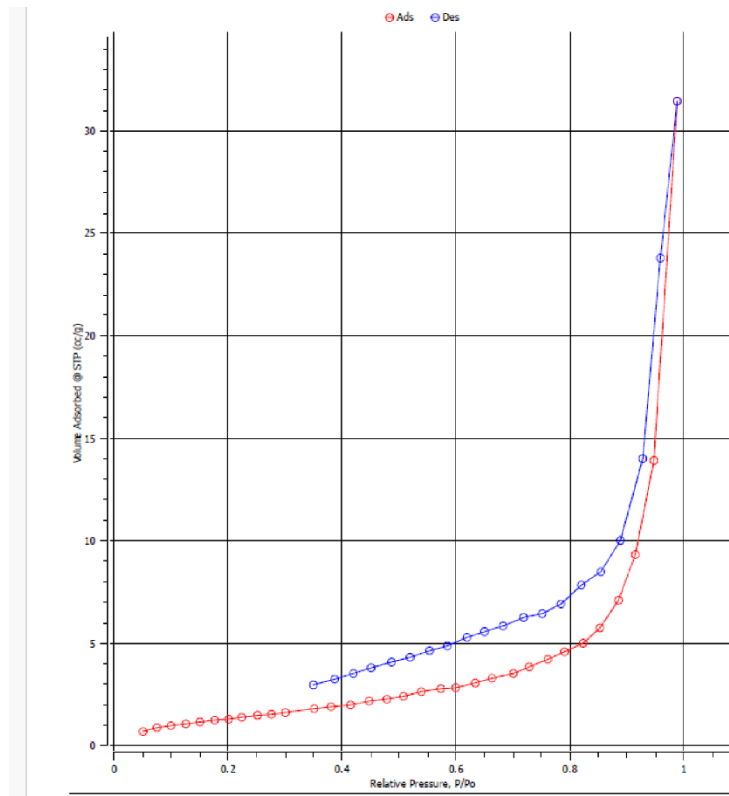

Fig. 7. DSC thermogram of iron NP
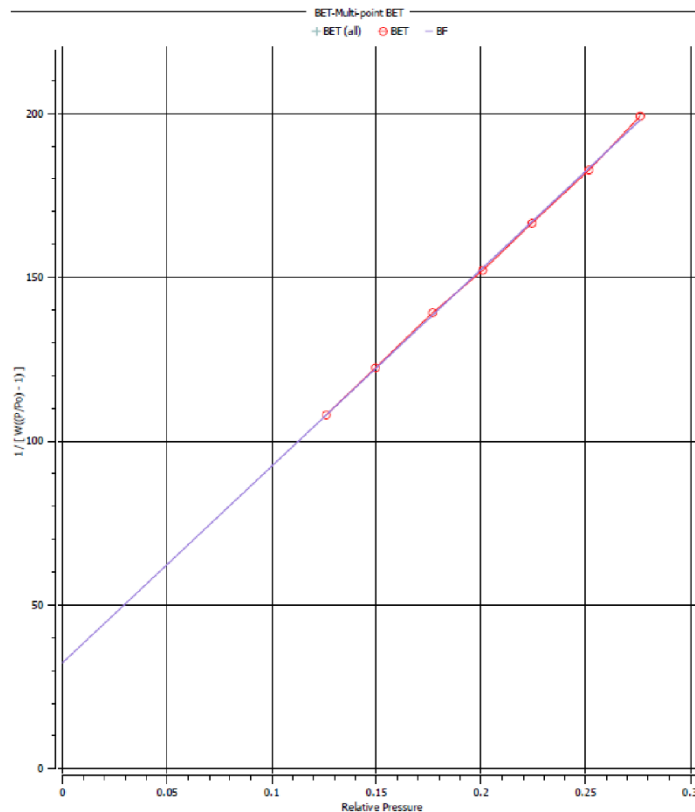
Fig. 8. BET adsorption isotherm- a

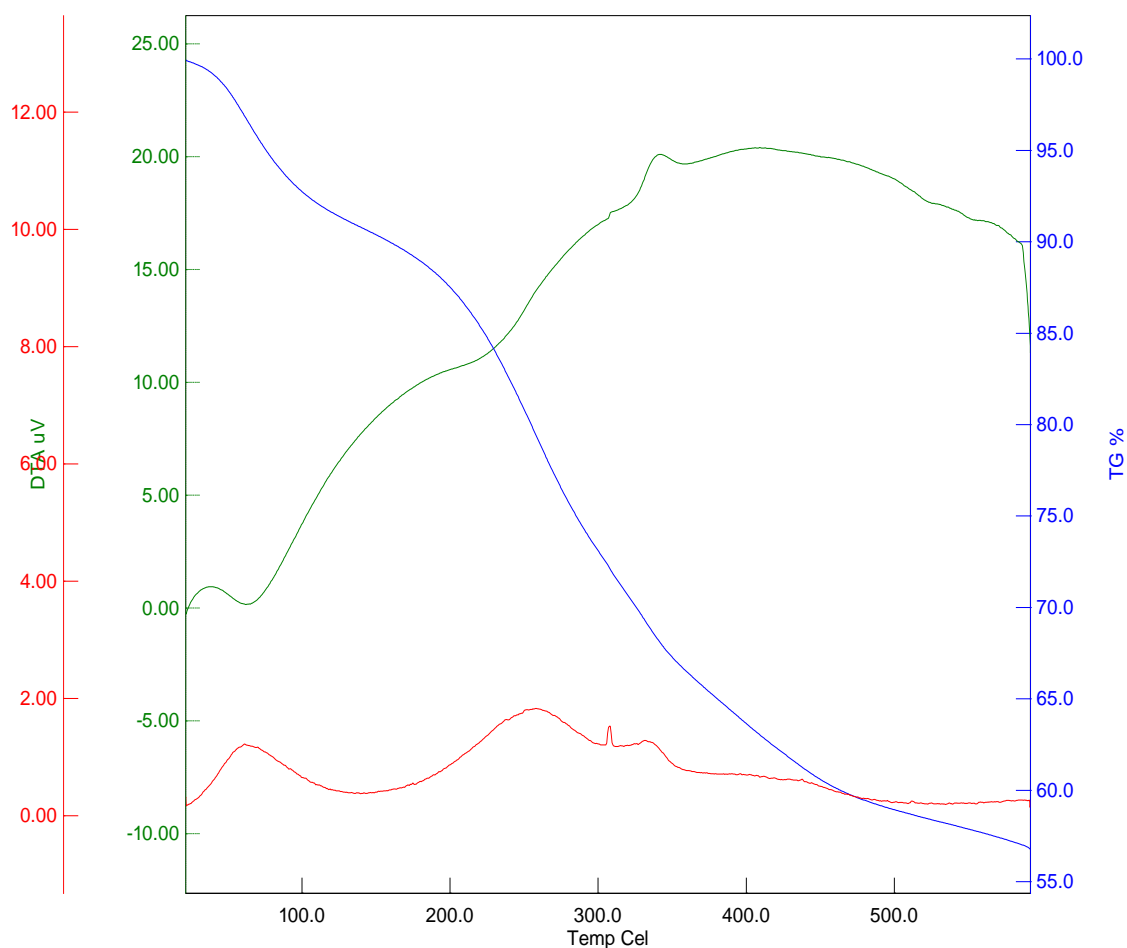**Fig. 9. BET adsorption isotherm - b**

Fig. 10. TGA curve (using *C. bicolor* extract synthesized via aqueous)

Table 1. FTIR spectrum of *C. bicolor*

Wave number (cm^{-1})	Functional group	Class
3682.85	O-H stretching	alcohol
3618.99	O-H stretching	alcohol
3026.21	C-H stretching	alkene
2917.08	C-H stretching	alkane
2649.38	O-H stretching	carboxylic acid
2212.71	C≡C stretching	alkyne
2020.52	N=C=S stretching	isothiocyanate
1980.35	C=C=C stretching	allene
1600.90	C=C stretching	conjugated alkene
1492.36	CH bending of CH$_2$	alkane
1451.72	C-H bending	alkane
1375.47	O-H bending	alcohol
1027.94	C-N stretching	amine
909.94	C-H bending	1,3-disubstituted
753.64	C-H bending	1,2-disubstituted
534.05	C-Br stretching	halo compound

47

Table 2. FTIR spectrum of NP

Wave number (cm^{-1})	Functional group	Class
3291.50	O-H stretching	alcohol
2919.20	C-H stretching	alkane
1628.11	C=C stretching	alkene
1415.79	S=O stretching	sulphate
1021.60	C-N stretching	amine
639.22	Fe-Cl stretching	halo compound

3.5 Thermogravimetric Analysis (TGA)

Thermal decomposition trend of the nanoparticle sample is shown in Fig. 10. The first weight loss is 5% and occurs between temperatures 25°C - 150°C, attributable to desorption of surface adsorbed molecules or solvents. This is followed by a 10% loss occurring as a result of a likely degradation of surface functionalized molecules and this occurs in the range of 150°C - 300°C. A 70% loss is recorded between 300°C and 500°C due to degradation of cross-linked molecules. A further 5% weight loss is recorded in the region of 450 - 500°C culminating in the degradation of residual molecules or char formation.

3.6 Fourier Transform Infrared (FTIR)

FTIR analysis was performed to confirm the formation of iron nanoparticles from iron (III) chloride and functional groups present in aqueous extract of *Caladium bicolor*.

The analysis shows O-H stretching indicative of alcohols in Table 1 (3682.85 cm^{-1}and 3618.99 cm^{-1}). As seen in Table 1, C-H bending at 909.94 cm^{-1} indicating a 1,3-disubstituted structure. CH bending of CH$_2$ (1492.36 cm^{-1}) and C-H bending (1451.72 cm^{-1}) confirm the presence of alkane structures in *C. bicolor*. In Table 2, O-H stretching (3291.50 cm^{-1}) is characteristic of alcohol functional group. Alkane is suspected due to C-H stretching at 2919.20 cm^{-1}, alkene due to C=C stretching at 1628.11 cm^{-1}. We suspect the band of iron (III) chloride vibrations at 639.22 cm^{-1} (Fe-Cl stretching).

4. CONCLUSION

The *Caladium bicolor* plant was successfully extracted and characterized with FTIR. Iron nanoparticles were successfully synthesized via aqueous extraction of *Caladium bicolor*. The synthesized NP was characterized using SEM, XRD, FTIR, DSC, TGA and BET. These all showed the successful synthesis of iron nanoparticles reduced and stabilized by *C. bicolor*. The efficiency of nanoparticle "bottom up" synthesis using *C. bicolor* has been established. This research also established that it required 10 mL *C. bicolor* extract and 90 mL 0.05M FeCl$_3$ solution to synthesize 0.20g of iron NP.

DISCLAIMER (ARTIFICIAL INTELLIGENCE)

Authors hereby declare that NO generative AI technologies such as Large Language Models (ChatGPT, COPILOT, etc.) and text-to-image generators have been used during the writing or editing of this manuscript.

COMPETING INTERESTS

Authors have declared that no competing interests exist.

REFERENCES

1. Christian P, Von der Kammer F, Baalousha M, Hofmann T. Nanoparticles: structure, properties, preparation and behaviour in environmental media. Ecotoxicology. 2008; 17:326-343.
2. Sukhanova A, Bozrova S, Sokolov P, Berestovoy M, Karaulov A, Nabiev I. Dependence of nanoparticle toxicity on their physical and chemical properties. Nanoscale Res Lett. 2018;13(44):2.
3. Talapin DV, Shevchenko EV. Introduction: Nanoparticle chemistry. Chem Rev. 2016; 116(18):1.
4. Ealia SAM, Saravanakumar MP. A review on the classification, characterization, synthesis of nanoparticles and their applications. IOP Conf Ser Mater Sci Eng. 2017;263:3-5.
5. Bhardwaj LK, Rath P, Choudhury M. A comprehensive review on the classification, uses, sources of nanoparticles (NPs) and their toxicity on health. Aerosol Sci Eng. 2023;7(1):69-86.
6. Modena MM, Ruhle B, Burg TP, Wuttke S. Nanoparticle characterization: What to measure? Adv Mater. 2019;31:1.
7. Ijaz I, Gilani E, Nazir A, Bukhari A. Detail review on chemical, physical and green synthesis, classification, characterization and applications of nanoparticles. Green Chem Lett Rev. 2020;13(3):223-224.
8. Mohamad AT, Kaur J, Sidik NAC, Rahman S. Nanoparticles: A review on their synthesis, characterization and

physicochemical properties for energy technology industry. J Adv Res Fluid Mech Therm Sci. 2018;46(1):2.

9. Quinson J, Jensen KM. From platinum atoms in molecules to colloidal nanoparticles: A review on reduction, nucleation and growth mechanisms. Adv Colloid Interface Sci. 2020;286:102300.

10. Harish V, Ansari MM, Tewari D, Yadav AB, Sharma N, Bawarig S, et al. Cutting-edge advances in tailoring size, shape and functionality of nanoparticles and nanostructures: A review. J Taiwan Inst Chem Eng. 2023;149:2.
Available:https://doi.org/10.1016/j.jtice.2023.105010

11. Cheng P, Zhang Y, Li M, Ma H, Xu W, Tan X, et al. Carbonaceous anodes and compatible exoelectrogens in high-performance microbial fuel cells: A review. ACS EST Eng. 2024;4(3):488-505.

12. Trivedi R, Upadhyay TK, Mujahid MH, Khan F, Pandey P, Sharangi AB, et al. Recent advancements in plant-derived nanomaterials research for biomedical applications. Processes. 2022;10(2):338.

13. Singh A, Singh NB, Hussain I, Singh H, Singh SC. Plant-nanoparticle interaction: An approach to improve agricultural practices and plant productivity. Int J Pharm Sci Invent. 2015;4(8):25-40.

14. Ahmad N, Sharma S, Singh VN, Shamsi SF, Fatma A, Mehta BR. Biosynthesis of silver nanoparticles from *Desmodium triflorum*: A novel approach towards weed utilization. Biotechnol Res Int. 2011;6.

15. Zhao X, Liu W, Cai Z, Han B, Qian T, Zhao D. An overview of preparation and applications of stabilized zero-valent iron nanoparticles for soil and groundwater remediation. Water Res. 2016;100:13.

Peer-review history:
The peer review history for this paper can be accessed here:
https://www.sdiarticle5.com/review-history/126031